A VB/MM View of the Identity S_N2 Valence-Bond State Correlation Diagram in Aqueous Solution†

Avital Sharir-Ivry and Avital Shurki‡,*

Department of Medicinal Chemistry and Natural Products, School of Pharmacy, The Lise Meitner-Minerva Center for Computational Quantum Chemistry, The Hebrew University of Jerusalem, Jerusalem 91120, Israel

Received: February 27, 2008

The valence-bond state correlation diagram (VBSCD), which was developed by Shaik and co-workers is an excellent tool to understand reactivity patterns in chemical reactions. The strength of the model is in its ability to describe the whole spectrum of reaction types and unify them under a single general paradigm. Moreover, it allows one to understand, conceptualize, and predict chemical reactivity in a general as well as specific manner. As such, VBSCD is a valuable model. The model has been largely tested on various systems in the gas phase both qualitatively and quantitatively. However, its application to reactions in solution was given less attention because of the difficulties to represent solvent reorganization and estimate non-equilibrium solvation effects, which, on the basis of the model, are expected to be fundamental. The recently developed valence-bond molecular mechanics (VB/MM) method overcomes these difficulties because it involves explicit solvent molecules and thus allows quantitative examination of these solvent effects. This work presents a study of the identity S_N2 reaction $X^- + H_3CX \rightarrow XCH_3 + X^-$; (X = F, Cl, Br, I) in aqueous solution. The various parameters that form the VBSCD model are calculated and compared with the corresponding model's estimated values. A relatively good agreement between the calculated and estimated values is found. It is shown that when facing quantitative considerations, the picture may not be as simplistic as in the qualitative study; yet, the fundamental nature of the description is unaffected. This indicates that combined together, the VB/MM approach and the VBSCD model offer a very powerful tool to study reactions in complex systems and understand their reactivity patterns.

Introduction

Over two decades ago, Shaik and co-workers have developed the valence-bond state correlation diagram (VBSCD) model.[1–8] At that time, the capabilities of quantum mechanics to calculate reaction energies, barriers, and other quantities, which define chemical reactivity, had already been recognized. What seemed to be missing was a model that would explain these phenomena and would answer fundamental questions such as why do reactions require activation energies in order to occur? What are the factors that govern the shape and height of these reaction barriers? What determines their selectivity? Shaik's VBSCD model addressed this deficiency.

The VBSCD model describes a barrier formation as a result of avoided crossing between two state curves: the reactants and the products, where each state can be a mixture of a few valence bond (VB) configurations (plain lines in Scheme 1).[9] As crossing is avoided, two new states are obtained (bold lines in Scheme 1): one that defines the ground state and another describing the system's excited state. By using the resulting diagram (Scheme 1), Shaik and co-workers formulated an expression for the reaction barrier $\Delta E^{\ddagger}$.[2–8] A simplified version is given here as a function of the three principal parameters of the model: G, the vertical gap between the reactant state, ψ_R(R), and the product's promoted state, ψ^*_P(R), at the reactant's geometry, f, the fraction of this gap that gives the height of E_c (the energy where the two states cross), and B, the energy gained by means of mixing of the two states (see also Scheme 1).

SCHEME 1: General VB State Correlation Diagram with Its Characteristic Parameters[a]

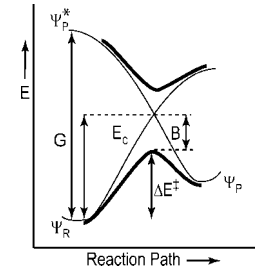

[a] The two diabatic states, reactants, ψ_R, and products, ψ_P, are in plain lines, and the resulting adiabatic states are in bold lines. G, E_c, and B present the promotion energy, the energy required for the two diabatic states to cross, and the resonance energy, respectively, and $\Delta E^{\ddagger}$ is the resulting activation barrier.

$$\Delta E^{\ddagger} = E_c - B = fG - B \qquad (1)$$

Finally, considering the chemical meaning underlying the VB wave functions, Shaik and co-workers elegantly assigned chemical meaning to these key parameters of the diagram. Thus, G was shown to be a function of the vertical charge-transfer energy in reactions where formal oxidation state changes and otherwise a function of the vertical singlet−triplet excitation energy. The quantity f, serving as a measure of the curvature of the diabatic curves, was shown to depend on several intrinsic properties of the system, such as the reaction free energy and

† Part of the "Sason S. Shaik Festschrift".

* Corresponding author: Email: avital@md.huji.ac.il. Phone: +972-2-675-8696. Fax: +972-2-675-7076.

‡ Affiliated with the David R. Bloom Center for Pharmacy at the Hebrew University.

10.1021/jp801722e CCC: $40.75
Published on Web 07/12/2008

the amount of delocalization, in the promoted states of the diagram. Finally, B, the resonance integral between the two states, was shown to incorporate symmetry characteristics of the wave functions. This, in turn, facilitated the understanding and assessment of the factors that control the barrier and therefore also allowed one to make predictions on different reactivity patterns (for more details see, for example, refs 2–8).

An impressive and colossal work of Shaik and co-workers throughout the years has demonstrated both the applicability and predictive power of the model for reactions in the gas phase (for reviews see, for example, refs 2–8 and references therein). It was initially established on the basis of empirical evaluations (for example, refs 2–4) and later was tested by using calculations (for example, refs 5–8 and 10–16). Reactions in condensed phase or in biological systems, on the other hand, were given relatively small attention.[17,18] The validation of the description of such reactions within the model was limited, until recently, to empirical estimations because VB computations for such complex systems were not available.

The increasing performance of computers in recent years has permitted the development of several ab initio VB-based methods which are able to calculate reactions in condensed phase and/or biological environment.[19–25] This created the opportunity to quantitatively examine the VBSCD model in such complex systems, and by now, several studies have attempted to calculate the various parameters of the VBSCD model.[26,27] These studies, however, involved the VBPCM approach, which describes the solvent by using a continuum model. Therefore, because of the inability of such a method to account for non-equilibrium solvation effects in the promoted state, both the energy gap, G, and the fraction, f, could not be fully calculated and were again estimated by using empirical derivations.

The recently developed hybrid valence-bond molecular mechanics (VB/MM) approach involves an explicit solvent model.[24] As such, it should be able to overcome the problem of non-equilibrium solvation and calculate the various parameters defining the VBSCD model without the aid of any additional derivations, thus, validating the model. This work presents a VB/MM study of the identity S_N2 reaction with different halides, while inspecting the various parameters of the VBSCD and examining their dependence on the identity of the halide. The calculated parameters are shown to agree well with previous estimations and predictions of the model, indicating that the model is an effective tool for the description of chemical reactions in solvents as well.

Methodology

VB/MM is a recently developed QM/MM method that combines ab initio VB with molecular mechanics calculations. As such, it divides the system into a reactive part and its surrounding, where the former is described with VB and the latter with MM. The VB/MM method has been described elsewhere;[24] hence, we will only give here a few key points.

The method describes reactions by mixing diabatic VB configurations. These configurations represent various arrangements of the reactive electrons that undergo major changes along the reaction. The resulting adiabatic potential energy surface is defined as the lowest eigenvalue of the following secular equations

$$\sum_{i}^{N}(H_{ij}-\varepsilon S_{ij})c_i=0 \tag{2}$$

where S_{ij} and H_{ij} are the overlap and Hamiltonian matrix elements, respectively, c_i are the coefficients of the respective VB configurations, Φ_i, in the overall wave function, and ε is the adiabatic energy.

The H_{ii} diagonal elements present the energy of the respective VB configuration Φ_i and are evaluated by the following equation

$$H_{ii}=H_{ii}^{0}+H_{ii}^{\mathrm{int}} \tag{3}$$

H_{ii}^{0} is the energy of VB configuration Φ_i of the isolated reactive fragments calculated at the QM level, whereas H_{ii}^{int} is the interaction energy of the same configuration with its surrounding, calculated classically.

The off-diagonal element, H_{ij}, is the resonance integral between VB configurations Φ_i and Φ_j. Its approximation is based on the assumption that the overlap and the reduced resonance integral are both invariant to the environment, leading to the following formulation:

$$H_{ij}=H_{ij}^{0}+\frac{1}{2}(H_{ii}^{\mathrm{int}}+H_{jj}^{\mathrm{int}})S_{ij}^{0} \tag{4}$$

where H_{ij}^{0} and S_{ij}^{0} present the resonance integral and the overlap between Φ_i and Φ_j calculated at the QM level for the isolated reactive fragments.

The quality of the results depends on a correct description of both the environment and the electronic structure of the reacting fragments, which affect each other. Thus, the system is allowed to relax and accommodate to some speculated electronic structure of the reacting fragments. The eigenvalue problem is then solved, and a new electronic structure is obtained. The process is then repeated until changes in the electronic structure are insignificant. This assures mutual polarization of the environment and the electronic structure of the reacting fragments.

Finally, the overall energy is given by

$$E_{\mathrm{VB/MM}}=\varepsilon+E(\mathrm{MM}) \tag{5}$$

where E(MM) accounts for the classical interactions of the environment within itself.

Computational Details

Quantum calculations were done by using the Gaussian[28] and XMVB[29,30] program packages for MO and VB calculations, respectively, whereas all the dynamics and force-field calculations employed the MOLARIS program package.[31,32] VB/MM calculations combine the two approaches and thus utilized an additional program which is responsible for the linkage between the two programs.

Quantum Calculations. Calculations employed the 6-31G(d) basis set for atoms C, H, F, and Cl and the Los-Alamos effective core potential with its matching basis set LANL2DZ[33] and additional d-polarization functions,[34] which were added to match the 6-31G(d) basis, was used for atoms Br and I. Gas-phase geometries of the reactants at infinite separation, reactants complex, and transition state (TS) for the various reacting fragments ($X^- + CH_3X$, X = F, Cl, Br, I) were obtained at the MP2 level of calculation. This level, together with the above basis sets, was shown to be satisfactory for these systems.[26] Other geometries along the reaction coordinate were obtained by dividing changes from reactants to the TS into 14 equal parts for F, Cl, and Br and 17 equal parts for I. These geometries were used also for the calculations in solution. The reaction barrier in the gas phase was calculated relative to the ion−molecule complex, whereas in solution, we continued slightly further along the reaction coordinate, until changes in energy were negligible.

VB calculations were carried out at the breathing orbital VB (BOVB) level which allows optimization of different orbitals for the different VB configurations.[35,36] The inner core electrons were frozen at the Hartree-Fock level, thereby leaving 22 valence electrons to be explicitly included in the VB calculations. Orbitals of all valence electrons were treated as "breathing orbitals".

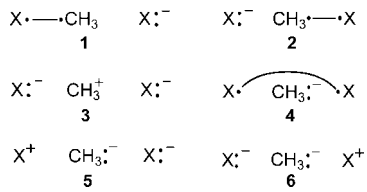

Six VB configurations are involved in the description of the S_N2 reaction (drawing **1**−**6**): two so-called covalent configurations as they describe the Heitler−London (HL) covalent bond of either the reactants, **1**, or the products, **2**; the principle ionic configuration, which involves a triple-ion arrangement with a carbocation and two halides, **3**; the long-bond (LB) configuration, which pairs the two electrons of the halogens (one on each atom), thus creating a covalent bond between them,**4**; and two additional ionic configurations which include a carbanion and a positively charged halogen, **5** and **6**. Previous calculations of the S_N2 reaction have shown that the three VB configurations **1**−**3** are adequate to describe the energetics of the adiabatic reaction profile because the other configurations were found to be negligible.[20,25,26,37] Thus, for simplicity, the adiabatic reaction profile was calculated by using only these three configurations **1**−**3**.

Calculations of the diabatic states, on the other hand, involved inclusion of the LB configuration, **4**, as well, because its contribution in the promoted state is expected to increase. Thus, the reactants and products diabatic states were described by configurations **1**, **3**, and **4** and **2**, **3**, and **4**, respectively. In order to keep the covalent character of these diabatic states in their unstable geometries (for example, keep the covalent character of the products C−X bond in $\psi_P^*(R)$), we were obliged to consider the second root of the Hamiltonian. However, because orbital optimization within XMVB can be done only for the first state, we first calculated the state while eliminating the ionic contributions. The resulting orbitals for both the covalent and the LB configurations served as guess orbitals for the full calculation of the diabatic state. The ionic orbitals were then taken from the adiabatic calculation, and the Hamiltonian was solved this time without allowing optimization of the orbitals. This process might affect the results by slightly underestimating the ionic contribution, but the overall trend should be correct. Finally, because these results are therefore not variational, they served only for the estimation of the weights of the various VB configurations. The calculations of the promotion energies involved the variational values obtained by eliminating the ionic contributions.

Classical Calculations. All simulations started with an initial guess for both the electronic structure of the reacting fragments and the geometric configuration of the solvent molecules. The system was then allowed to relax while both the geometry and the electronic structure of the reacting fragments were fixed, letting the solvent molecules accommodate to the reacting fragments state. A single-point VB/MM calculation was then carried out, and the newly obtained electronic structure of the reacting fragments expressed as new weights for the diabatic configurations was compared to the preceding one. The process was repeated with the new electronic structure until convergence was achieved (difference of up to 0.05 in the weights between sequential relaxations). Once converged, various solvent configurations were collected (50 for the reactions with X = F, Cl and 100 for reactions with X = Br, I) for each geometry of the reacting fragments along the reaction coordinate. This was done by continuously equilibrating the system at each solute geometry and performing a VB/MM calculation after every 0.8−1 ps in simulation that spanned an overall 50 or 100 ps. Finally, the overall energetics was obtained by using potential of mean force (PMF) calculations[38–41] combined with the free energy perturbation (FEP) procedure.[42,43] All the simulations were carried out at 300K and involved 1 fs time step.

The simulation system was divided into four regions: region I included the reacting fragments methyl halide and the halide anion ($CH_3X + X^-$); region II included the water molecules up to a radius of 18 Å; and region III included water molecules that were subjected to distance and polarization constraints according to the surface-constrained all atom solvent boundary condition.[44] The rest of the system was presented by a bulk region with a dielectric constant of 80. The long-range electrostatic effects were treated by the local reaction field method.[45] Molecular mechanics calculations utilized the ENZYMIX force field.[31,32] A detailed description of the force-field parameters for the reacting fragments at the various VB configurations is given in the Supporting Information.

The PMF curves seem to fall short in predicting the accurate energy rise in the diabatic states as they extend over a large energy range. As a result, the relative energies between the various VB states as predicted by the PMF curves are underestimated. Therefore, the values of the promotion gap, *G*, and the resonance integral, *B*, were taken as an averaged energy difference between different single-point calculations at the respective geometries rather than as the energy difference between the corresponding PMF curves. We note in this respect that a better accuracy within the PMF scheme could be achieved by increasing the number of FEP steps; however, because our interest was in only two geometries, it seemed unnecessary.

Results and Discussion

The reactions chosen for this study are the following identity S_N2 reactions with halides serving as nucleophiles:

$$X^- + CH_3X \rightarrow XCH_3 + X^- \qquad (X = F, Cl, Br, I) \qquad (6)$$

This reaction occurs with no thermodynamic driving force and thus serves as an excellent starting point for inspection of the various parameters of the model. It reduces the added complexity caused by reaction energy and allows for the examination of the model in its most simplified version. Additionally, it was characterized and studied extensively within the model.[3,13,17,18,26,46–48]

In order to examine the various parameters of the VBSCD model and their physical meaning, it is essential to have reasonable potential energy surfaces. Table 1 lists our calculated reaction barriers for different halides and compares the results to experimental data whenever available. The first two columns consider the gas-phase values. We chose the BOVB level of calculation that was shown to give reasonable values in an earlier study of these systems.[26] Our calculations, however, differing from the earlier study, involved only the three principle VB configurations **1**−**3** rather than all six configurations. By looking at the table, we can see that there is a relatively good agreement

TABLE 1: Calculated and Experimental S_N2 Reaction Barriers for Different Halides Both in Gas Phase and in Solution[a]

	gas phase		solution	
X	$\Delta E^{\ddagger}_{calc}$	$\Delta E^{\ddagger}_{exp}$	$\Delta E^{\ddagger}_{calc}$	$\Delta E^{\ddagger}_{exp}$[e]
F	14	~11[b]	28.2	31.8
Cl	9.9	10.2[c]	26.0	26.5
Br	9.5	11.2[c]	25.1	23.7
I	7.9	6.4[d]	21.1	23.2

[a] Energies are in kcal/mol. Gas-phase values are calculated at the BOVB/6-31G* level, whereas solution values are given at the (BOVB/6-31G*)/MM level of calculation. [b] Based on estimations from experimental data.[49] [c] Taken from ref 50 and 51. [d] Estimation taken from ref 46. [e] Experimental values are taken from ref 52.

TABLE 2: Computed VBSCD Parameters for the S_N2 Reaction in Gas Phase and in Aqueous Solution[a]

	G^b	f	B^b	$\Delta E_c{}^b$
		Gas		
F	234	0.175	27	41
Cl	167	0.168	18	28
Br	147	0.190	18	28
I	112	0.223	17	25
		Solution		
F	392	0.122	20	48
Cl	324	0.136	18	44
Br	270	0.144	14	39
I	217	0.171	16	37

[a] Gas-phase values are calculated at the BOVB/6-31G* level, whereas solution values are given at the (BOVB/6-31G*)/MM level of calculation. [b] Energies are in kcal/mol.

with the experimental data, suggesting that these three VB configurations suffice to properly describe the energetics of the system.

Any polar solvent is expected to increase the reaction barrier in these systems. The last two columns of Table 1 present the reaction barriers in solution. Calculated values are based on the BOVB/MM level of calculation. By looking at the results, we find good agreement with the experimental data, suggesting that VB/MM succeeds to produce the proper increase in energy due to the solvent. Moreover, because VB/MM utilizes explicit water molecules, the method can capture the reorganization and the non-equilibrium effects of the solvent.

Our goal is to follow the VBSCD model for solvated systems and evaluate its underlying parameters while comparing to earlier estimations, interpretations, and predictions. Table 2 presents the calculated parameters both in gas phase and in solution.

We note in that respect that when calculating the diabatic states, throughout the reaction coordinate, we found that the most stable combination changed its character, similar to earlier findings.[13] Namely, for example, in the case of the so-called covalent diabatic state, which involves a linear combination of configurations **1**, **3**, and **4**, the most stable combination in the reactants' geometry involves a major covalent contribution. Yet, at the products geometry, usually, the ionic contribution became dominant in the most stable combination, entirely changing the character of the state. Because our interest remained the diabatic state, which presents a covalent bond as in the reactants, we considered the second root of the Hamiltonian, which usually was more appropriate, and defined our state of interest while keeping the general characteristics of the state with which we started. The various G values are therefore calculated relative to this state.

SCHEME 2: Reactant State, $\psi_R(R)$ and Product Promoted State, $\psi^*_P(R)$ at the Reactant's Geometry for the Identity S_N2 Reaction[a]

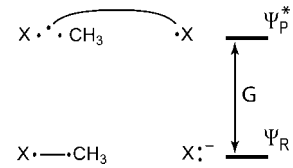

[a] Dots represent the electrons, and lines connecting them represent bond pairing of these electrons.

By looking at the table, we find that the values obtained for the systems in the gas phase are somewhat different than earlier reported results.[26] This difference stems from differences in the BOVB levels utilized in the two cases, which involve both different number of VB configurations and different numbers of orbitals optimized within the BOVB. Yet, the divergence is relatively small, and in both cases, the same trend is obtained. Thus, the promotion energy, G, is large and decreases by following the order F > Cl > Br > I. The fraction of the promotion gap that enters under the crossing point, f, changes to a much lesser extent, slowly increasing along the column, whereas the resonance energy, B, is the largest for X = F and somewhat smaller for the remaining halogens.

For the solution, it is seen that the promotion energies, G, largely increased, whereas both the fraction f, and the resonance energy, B, decreased compared to their respective values in the gas phase. Comparison to the earlier reported results in solution,[26] we find large differences both in the actual values and in some cases also in the overall trend. Our results are based on the VB/MM methodology, which involves explicit water molecules, whereas the previously calculated parameters were calculated with the VBPCM method, where the solvent molecules are considered implicitly via a continuum model. Therefore, as stated before, our calculations should fully account for both solvent reorganization and the resulting non-equilibrium solvation effects, which are only partially accounted for with the VBPCM. Because these two solvent effects are crucial to obtain correct values of the various VBSCD parameters, our results should give a better description for the model.

We can therefore discuss each one of the model's parameters and compare to Shaik's earlier predictions. Note that, in so doing, we will refer to the simplistic model described by eq 1, which is sufficient for identity S_N2 reaction because of the absence of reaction energy.

Promotion Energy Gap, *G*. The promotion energy gap, G, is the energy difference between the reactant and the product states in the geometry that corresponds to the reactants (see Scheme 1). In the S_N2 reaction, the VBSCD model predicts this gap to be a measure of the donor potency of the nucleophile $X:^-$ relative to the acceptor strength of the H_3C-X bond, because it involves an electron shift between these two species (see Scheme 2) and hence can be determined as follows:

$$G = I^*_{X:^-} - A^*_{CH_3X} \tag{7}$$

where $I^*_{X:^-}$ and $A^*_{CH_3X}$ are the vertical ionization potential of $X:^-$ and electron affinity of H_3C-X, respectively.

An additional interpretation that can be given to the promotion gap illustrated in Scheme 2 is the breaking of a bond between the leaving group and the methyl group followed by three-electron repulsion, which is developed between the two. Translating this into quantum mechanical expressions, Shaik and co-workers have demonstrated that these two quantities can

TABLE 3: Promotion Energy Gap, *G*, Estimated on the Basis of Interpretations of the Model[a]

	G_g[b]	G_s[c]
F	216	354
Cl	167	261
Br	140	233
I	112	195

[a] Energies are in kcal/mol. [b] Estimated by using eq 8 where bond energies are taken from ref 53 for X = F, Cl, I and from ref 54 for X = Br. [c] Estimated by using eq 10 with G_g values taken from our BOVB/6-31G(d) calculations, the solvent reorganization factor, ρ, is estimated to be 0.56 for water, and S_{X^-} values are taken from experiment, Table 5.10 in ref 55 and ref 56 (see also Supporting Information).

be approximated by the same expression, suggesting that the gas-phase gap can be estimated as twice the bond energy of the H_3C-X bond.[6]

$$G \approx 2D(C-X) \tag{8}$$

The first column of Table 3 lists the bond energy of C−X multiplied by two. Comparing the calculated values of *G* (Table 2, entries 1−4) to the estimated ones, one finds, as was shown earlier,[26] a relatively good agreement, suggesting that the model's predictions are good.

For solution, one has to account for the various effects of the solvent. The promotion energy, *G*, is defined as the vertical excitation energy between the reactant and the product states in the reactants' geometry. When solvent is involved, the orientation of the solvent molecules in the promoted state should, therefore, also retain the original orientation that they possess in the reactant state. Consequently, the species in the promoted state should be considered under conditions of non-equilibrium solvation, where reorganization of the solvent molecules to the new electronic arrangement does not take place. Thus, on the basis of the model, the difference between the promotion energy in solution, G_s, relative to that in the gas phase, G_g, arises from the differential desolvation of the reacting species in their reactant and product electronic states, $S[\psi_R(R)]$ and $S^*[\psi^*_P(R)]$, respectively, both in the reactant's geometry.

$$G_s \approx G_g + S[\psi_R(R)] - S^*\left[\psi^*_P(R)\right] \tag{9}$$

Whereas the reactant state, $\psi_R(R)$, is expected to largely stabilize as a result of the solvation of $X:^-$, the promoted state, $\psi^*_P(R)$, is expected to stabilize to a lesser extent because it involves non-equilibrium solvation of the $(H_3C-X)^-$ species. Thus, overall, the promotion energy in solution is expected to increase.

$S^*[\psi^*_P(R)]$ presents a non-equilibrium desolvation and is therefore hard to estimate, because it represents desolvation energy that does not involve the reorganization effect of the solvent molecules. Shaik has shown a way to bypass this difficulty by approximating the reorganization energy as a fraction, ρ, of the corresponding solvation energies.[17,57] Additionally, he further simplified the expression by utilizing the VBSCD model to expand the electronic structure and the resulting desolvation energies of $(R-X)^-$ into components which are easier to evaluate, while neglecting contributions of, for example, the carbanion's desolvation $S_{R:^-}$, which are assumed to be small. The resulting expression derived by Shaik is given in eq 10:[17]

$$G_s \approx G_g + 2\rho S_{X:^-} \tag{10}$$

The second column of Table 3 lists the promotion energies in aqueous solution G_s, estimated by eq 10. By comparing the estimated values with the values obtained within the VB/MM calculations (Table 2 entries 5−8), we find that the calculated ones are somewhat larger than the estimations. Derivation of eq 10 involved several approximations, such as, disregarding the fact that G_g is measured at the geometry of the ion−molecule complex whereas G_s is measured for the species at infinite separation, approximating the reorganization energies, neglecting desolvation contributions of several species, and so forth. These various approximations may result in underestimation of the promotion gap. In our calculations, on the other hand, evaluation of the energies of the promoted state involved two VB configurations rather than the three that are believed to contribute (see Computational Details). Thus, our calculated promotion energies are likely to be overestimated. Consequently, the actual promotion energies are expected to be somewhere between the calculated and the estimated values, suggesting that the estimations are reasonable. Finally, overall, the model predicts the promotion energy to be the dominant quantity in the determination of the barrier height in the identity S_N2 reaction. Comparing the promotion energies in solution, G_s, to the gas-phase promotion energies, G_g (Table 2), it is seen that the promotion energies have indeed increased considerably as predicted by the model, leading to the increase in the reaction barriers. Furthermore, the promotion energies, G_s, are shown to decrease according to the following order F > Cl > Br > I, which is the same trend observed for the respective reaction barriers.

Fraction of the Gap Under the Barrier, *f*. *f* is the fraction of the promoted gap, *G*, that actually enters under the barrier. It is determined by the curvature of the diabatic curves, where a steep decent of the promoted state, ψ^*_P, along the reaction coordinate from the reactants geometry towards the crossing point would lead to a small value of *f* and visa versa. Shaik and co-workers, who realized that it is bond ionicity in the diabatic states that determines the curvature, assigned a chemical meaning to the fraction *f*, suggesting that it measures the amount of delocalization of the electrons in the promoted state.[6,46] By following these predictions, electronic delocalization in the promoted states will be associated with larger *f* values and thus, for cases with identical promotion gap, a higher barrier.

Considering the S_N2 reaction, the principle character of the promoted state at the reactant geometry should be the products' HL (covalent) configuration, ϕ^P_{cov}. However, because of electronic delocalization, the promoted state should be a mixture of ϕ^P_{cov}, with both the long bond, ϕ_{LB}, and the triple ionic, ϕ_{ION}, configurations, (see Scheme 3).

The overall bond ionicity, ω_{del} in Scheme 3, which is the sum of the contributions of both ϕ_{ION} and ϕ_{LB}, should serve in that case as a measure of the amount of delocalization. *f*, therefore, is predicted by the VBSCD model to be proportional to ω_{del}. More specifically, large ω_{del} values, which reflect large delocalization, should be followed by large values of *f* and visa versa. In order to examine this prediction, Table 4 shows the weights of the various configurations in the promoted state, both in gas phase and in solution. The values of the overall bond ionicity are also listed as the delocalization weight, ω_{del}.

By looking at the delocalization weights and comparing them to the values of *f* both in gas phase and in solution, one finds nice correlations. It is seen that both ω_{del} and *f* show the same trend, being smallest for X = F and increasing down the column (that is, F < Cl < Br < I), both in the gas phase and in solution. Furthermore, when moving from gas phase to solution, systems are expected to favor charge localization, and indeed, both the

SCHEME 3: Electronic Delocalization within the Promoted State, Where ω^{P}_{cov}, ω_{ION}, and ω_{LB} Represent the Contributions of ϕ^{P}_{cov}, ϕ_{ION}, and ϕ_{LB}, Respectively, to the Overall Promoted State, and ω_{del} Represents the Overall Delocalization

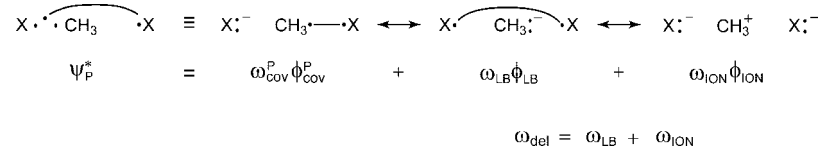

TABLE 4: Weight of the Various Configurations That Contribute to the Promoted State along with the Overall Delocalization Both in Gas Phase and Solution for the Different Halides

	gas phase[a]		solution[b]	
X	$\omega^{P}_{cov}/\omega_{LB}/\omega_{ION}$	ω_{del}	$\omega^{P}_{cov}/\omega_{LB}/\omega_{ION}$	ω_{del}
F	0.600/0.234/0.166	0.400	0.700/0.265/0.035	0.300
Cl	0.491/0.255/0.254	0.509	0.594/0.385/0.021	0.406
Br	0.422/0.224/0.354	0.578	0.569/0.380/0.051	0.431
I	0.357/0.213/0.430	0.643	0.463/0.415/0.121	0.536

[a] Calculated at the ion−molecule complex geometry. [b] Calculated at the geometry where the distance between the species energetically resembles infinite separation.

overall delocalization weights and the values of *f* decrease when moving to solution.

We note, in that respect, that earlier descriptions of the delocalization effect of the promoted state involved consideration of only the long bond contributions, while neglecting the contributions of the triple-ionic configurations(for example, refs 17 and 46). Thus, the predictions based on this description involved a correlation between ω_{LB} and the value of *f*. By looking at the values of ω_{LB} (Table 4) and comparing them to the values of *f* (Table 2), no obvious correlation can be found. This, however, should not be interpreted as a fault of the model, because it is only a result of an oversimplification of the delocalization effect by the model.

These results suggest that quantitatively, things can be a little bit more complex than one wishes. Yet, the essence of the idea, interpretation, and predictions of the model remain valid.

Resonance Energy of the TS, *B*. The last parameter is the stabilization of the adiabatic state at the TS geometry relative to the crossing point of the two diabatic states, referred to as the resonance energy, *B*. This parameter measures the avoided crossing interaction and is suggested by the VBSCD model to be related to the bond strength or the singlet−triplet excitation energy of the active bonds in the TS.

The recent work by Shaik and co-workers nicely studied the parameter *B* for the identity S_N2 reaction both in gas and solution and examined the relation between the calculated values and the values estimated by the model.[26] Comparison of the resonance energies obtained by us (Table 2) to those obtained by Shaik and co-workers (Tables 7 and 8 in ref 26) reveals great similarity, both in the trends and (although to a lesser extent) in the absolute values. This result was anticipated because non-equilibrium solvation effects on the TS resonance energy are expected to be small. Hence, in this case, our VB/MM calculations have no obvious advantage over the VBPCM, and the results are therefore expected to be similar. We note in this respect that the differences between our results and the results obtained in the VBPCM study originate from the different numbers of VB configurations that were considered in the calculations.

Therefore, in order to avoid repetition, we will not elaborate on the resonance energy, *B*, and will only point out that by following the model's predictions, *B* was found to nicely correlate with the contribution of the ionic configuration, ϕ_{ION}, in the TS, where large ionic contributions lead to small values of *B* and visa versa. Therefore, because overall, the solvent increased the ionic contribution, the values of *B* decreased compared to those in the gas phase.

Concluding Remarks

We studied the identity S_N2 reaction with a series of halides in aqueous solution by using the VB/MM method, and different aspects of the VBSCD model were examined quantitatively. VB/MM was shown to be a useful tool for calculating the parameters of the VBSCD. It is a hybrid method that involves explicit solvent molecules. As such, it can account for non-equilibrium solvation effects, which are important for the calculation of some of the VBSCD parameters and thus was shown to succeed where other methods have failed.

The VBSCD model was analyzed quantitatively. It was found that in some cases the quantitative description is somewhat less simplistic than the qualitative one; yet, overall, the ideas as well as the conclusions are kept. Furthermore, good agreement was found between the calculated values and those estimated on the basis of the model, suggesting that the predictive power of the model is very good.

The strength of the VBSCD model is in its ability to describe any reaction by the same general simplistic patterns while capturing the entire physical meaning of the problem, thus contributing to the understanding. Our results are therefore encouraging because they suggest that an interplay between the accurate calculations and the qualitative model is possible. This, in turn, should enable understanding of reactions in complex systems, such as proteins, where intuition is somewhat lost. In such systems, it is usually hard to predict, for example, what would be the so-called solvation effect because they are multifaceted. However, the ability to calculate the parameters and then use the model to understand the numbers obtained should shed light on the systems, resulting with a better understanding, and this is the scope of our future studies.

Acknowledgment. The paper is dedicated to Prof. Sason Shaik, a remarkable man and a great teacher, who introduced us into the realm of the VB theory and captured us by the charms of its simplicity and beauty. The research was partially supported by The Israel Science Foundation (Grants No. 1317/05 and 1320/05) and by the Human Frontiers of Science Program HSFP (Grant No. RGY0068/2006-C102).

Supporting Information Available: It includes force-field parameters of the reacting fragments in the various VB configurations and the solvation energies of the various halides. This material is available free of charge via the Internet at http://pubs.acs.org.

References and Notes

(1) Shaik, S. S. *J. Am. Chem. Soc.* **1981**, *103*, 3692.
(2) Pross, A.; Shaik, S. S. *Acc. Chem. Res.* **1983**, *16*, 363.

(3) Shaik, S. S. *Prog. Phys. Org. Chem.* **1985**, *15*, 197.
(4) Shaik, S. S. A Qualitative Valence Bond Approach to Organic Reactions. In *New Theoretical Concepts for Understanding Organic Reactions NATO ASI Series*; Bertran, J., Csizmadia, G. I., Eds.; Kluwer: Dordrecht, Holland, 1989; Vol. C267.
(5) Shaik, S. S.; Hiberty, P. C. Curve Crossing Diagrams as General Models for Chemical Reactivity and Structure. In *Theoretical Concepts for Chemical Bonding*; Maksic, Z. B., Ed.; Springer-Verlag, 1991; Vol. 4; pp 269.
(6) Shaik, S.; Hiberty, P. C. Valence bond mixing and curve crossing diagrams in chemical reactivity and bonding. In *Advances in Quantum Chemistry*, 1995; Vol. 26; pp 99.
(7) Shaik, S.; Shurki, A. *Angew. Chem., Int. Ed.* **1999**, *38*, 586.
(8) Shaik, S.; Hiberty, P. C. *Rev. Comput. Chem.* **2004**, *20*, 1.
(9) It is noted that a complementary development of the model involves the VB configuration-mixing diagram VBCMD which considers the contribution of each VB configuration separately and can, therefore, describe also stepwise reactions.
(10) Sini, G.; Shaik, S. S.; Lefour, J. M.; Ohanessian, G.; Hiberty, P. C. *J. Phys. Chem.* **1989**, *93*, 5661.
(11) Maitre, P.; Hiberty, P. C.; Ohanessian, G.; Shaik, S. S. *J. Phys. Chem.* **1990**, *94*, 4089.
(12) Sini, G.; Ohanessian, G.; Hiberty, P. C.; Shaik, S. S. *J. Am. Chem. Soc.* **1990**, *112*, 1407.
(13) Sini, G.; Shaik, S.; Hiberty, P. C. *J. Chem. Soc., Perkin Trans. 2* **1992**, 1019.
(14) Shaik, S.; Reddy, A. C. *J. Chem. Soc., Faraday Trans.* **1994**, *90*, 1631.
(15) Song, L. C.; Wu, W.; Dong, K.; Hiberty, P. C.; Shaik, S. *J. Phys. Chem. A* **2002**, *106*, 11361.
(16) Wu, W.; Shaik, S.; Saunders, W. H. *J. Phys. Chem. A* **2002**, *106*, 11616.
(17) Shaik, S. S. *J. Am. Chem. Soc.* **1984**, *106*, 1227.
(18) Shaik, S. S. *Isr. J. Chem.* **1985**, *26*, 367.
(19) Mo, Y. R.; Gao, J. L. *J. Phys. Chem. A* **2000**, *104*, 3012.
(20) Mo, Y. R.; Gao, J. L. *J. Comput. Chem.* **2000**, *21*, 1458.
(21) Song, L. C.; Wu, W.; Zhang, Q.; Shaik, S. *J. Phys. Chem. A* **2004**, *108*, 6017.
(22) Hong, G. Y.; Rosta, E.; Warshel, A. *J.Phys. Chem. B* **2006**, *110*, 19570.
(23) Wesolowski, T. A.; Warshel, A. *J. Phys. Chem.* **1993**, *97*, 8050.
(24) Shurki, A.; Crown, H. A. *J. Phys. Chem. B* **2005**, *109*, 23638.
(25) Sharir-Ivry, A.; Crown, H. A.; Wu, W.; Shurki, A. *J. Phys. Chem. A* **2008**, *5*, 2489.
(26) Song, L. C.; Wu, W.; Hiberty, P. C.; Shaik, S. *Chem. Eur. J.* **2006**, *12*, 7458.
(27) Su, P. F.; Ying, F. M.; Wu, W.; Hiberty, P. C.; Shaik, S. *ChemPhysChem* **2007**, *8*, 2603.
(28) Frisch, M. J.; Trucks, G. W.; Schlegel, H. B.; Scuseria, G. E.; Robb, M. A.; Cheeseman, J. R.; Montgomery, J. A., Jr.; Vreven, T.; Kudin, K. N.; Burant, J. C.; Millam, J. M.; Iyengar, S. S.; Tomasi, J.; Barone, V.; Mennucci, B.; Cossi, M.; Scalmani, G.; Rega, N.; Petersson, G. A.; Nakatsuji, H.; Hada, M.; Ehara, M.; Toyota, K.; Fukuda, R.; Hasegawa, J.; Ishida, M.; Nakajima, T.; Honda, Y.; Kitao, O.; Nakai, H.; Klene, M.; Li, X.; Knox, J. E.; Hratchian, H. P.; Cross, J. B.; Bakken, V.; Adamo, C.; Jaramillo, J.; Gomperts, R.; Stratmann, R. E.; Yazyev, O.; Austin, A. J.; Cammi, R.; Pomelli, C.; Ochterski, J. W.; Ayala, P. Y.; Morokuma, K.; Voth, G. A.; Salvador, P.; Dannenberg, J. J.; Zakrzewski, V. G.; Dapprich, S.; Daniels, A. D.; Strain, M. C.; Farkas, O.; Malick, D. K.; Rabuck, A. D.; Raghavachari, K.; Foresman, J. B.; Ortiz, J. V.; Cui, Q.; Baboul, A. G.; Clifford, S.; Cioslowski, J.; Stefanov, B. B.; Liu, G.; Liashenko, A.; Piskorz, P.; Komaromi, I.; Martin, R. L.; Fox, D. J.; Keith, T.; Al-Laham, M. A.; Peng, C. Y.; Nanayakkara, A.; Challacombe, M.; Gill, P. M. W.; Johnson, B.; Chen, W.; Wong, M. W.; Gonzalez, C.; Pople, J. A. *Gaussian 03*, revision B.04; Gaussian, Inc.: Wallingford, CT, 2004.
(29) Song, L. C.; Wu, W.; Mo, Y.; Zhang, Q. *XMVB-0.1 - An ab initio Non-Orthogonal Valence Bond Program* ; Xiamen University: Xiamen , 2003.
(30) Wu, W.; Mo, Y.; Cao, Z.; Zhang, Q. A Spin Free Approach for Valence Bond Theory and Its Application. In *Valence Bond Theory*; Cooper, D. L., Ed.; Elsevier: Amsterdam, 2002; pp 143.
(31) Chu, Z. T.; Villa, J.; Štrajbl, M.; Schutz, C. N.; Shurki, A.; Warshel, A. *MOLARIS version beta9.05*; University of Southern California: Los Angeles, 2004; in preparation.
(32) Lee, F. S.; Chu, Z. T.; Warshel, A. *J. Comput. Chem.* **1993**, *14*, 161.
(33) Hay, P. J.; Wadt, W. R. *J. Chem. Phys.* **1985**, *82*, 299.
(34) Check, C. E.; Faust, T. O.; Bailey, J. M.; Wright, B. J.; Gilbert, T. M.; Sunderlin, L. S. *J. Phys. Chem. A* **2001**, *105*, 8111.
(35) Hiberty, P. C.; Flament, J. P.; Noizet, E. *Chem. Phys. Lett.* **1992**, *189*, 259.
(36) Hiberty, P. C.; Shaik, S. Breathing-Orbital Valence Bond - A Valence Bond Method Incorporating Static and Dynamic Electron Correlation Effects. In *Valence Bond Theory*; Cooper, D. L., Ed.; Elsevier: Amsterdam, 2002; pp 187.
(37) Hwang, J.-K.; King, G.; Creighton, S.; Warshel, A. *J. Am. Chem. Soc.* **1988**, *110*, 5297.
(38) King, G.; Warshel, A. *J. Chem. Phys.* **1990**, *93*, 8682.
(39) Burkert, U.; Allinger, N. L. *Molecular Mechanics*; American Chemical Society: Washington D. C., 1982.
(40) Roux, B. *Comput. Phys. Commun.* **1995**, *91*, 275.
(41) Muller, R. P.; Warshel, A. *J. Phys. Chem.* **1995**, *99*, 17516.
(42) Zwanzig, R. W. *J. Chem. Phys.* **1954**, *22*, 1420.
(43) Valleau, J. P.; Torrie, G. M. *Modern Theoretical Chemistry*; Plenum Press: New York, 1977; Vol. 5, p 169.
(44) King, G.; Warshel, A. *J. Chem. Phys.* **1989**, *91*, 3647.
(45) Lee, F. S.; Warshel, A. *J. Chem. Phys.* **1992**, *97*, 3100.
(46) Shaik, S. S.; Pross, A. *J. Am. Chem. Soc.* **1982**, *104*, 2708.
(47) Shaik, S. S. *New J. Chem.* **1982**, *6*, 159.
(48) Shaik, S. S.; Schlegel, H. B.; Wolfe, S. *Theoretical Aspects of Physical Organic Chemistry: The Sn2 Mechanism*; Wiley-Interscience: New-York, 1992.
(49) Depuy, C. H.; Gronert, S.; Mullin, A.; Bierbaum, V. M. *J. Am. Chem. Soc.* **1990**, *112*, 8650.
(50) Pellerite, M. J.; Brauman, J. I. *J. Am. Chem. Soc.* **1980**, *102*, 5993.
(51) Pellerite, M. J.; Brauman, J. I. *J. Am. Chem. Soc.* **1983**, *105*, 2672.
(52) Albery, W. J.; Kreevoy, M. M. *Adv. Phys. Org. Chem.* **1978**, *16*, 87.
(53) Benson, S. W. *J. Chem. Educ.* **1965**, *42*, 502.
(54) Ferguson, K. C.; Okafo, E. N.; Whittle, E. *J. Chem. Soc., Faraday Trans. I* **1973**, *69*, 295.
(55) Marcus, Y. *Ion Solvation*; John Wiley and Sons: New-York, 1985.
(56) Zhan, C. G.; Dixon, D. A. *J. Phys. Chem. A* **2004**, *108*, 2020.
(57) Delahay, P. *Acc. Chem. Res.* **1982**, *15*, 40.

JP801722E